PERGAMON

International Journal of Heat and Mass Transfer 45 (2002) 2439–2447

International Journal of HEAT and MASS TRANSFER

www.elsevier.com/locate/ijhmt

Thermal conductivity of amorphous silicon thin films

Seungjae Moon [a], Mutsuko Hatano [a,b], Minghong Lee [a], Costas P. Grigoropoulos [a,*]

[a] *Department of Mechanical Engineering, University of California, Berkeley, CA 94720-1740, USA*
[b] *Central Research Laboratory, Hitachi Ltd., Tokyo 185-8601, Japan*

Received 26 January 2001; received in revised form 09 November 2001

Abstract

The thermal conductivity of amorphous silicon thin films is determined by using the non-intrusive, in situ optical transmission measurement as well as by the 3ω method. The temperature dependence of the film complex refractive index is determined by spectroscopic ellipsometry. The acquired transmission signal is fitted with predictions obtained by coupling conductive heat transfer with multi-layer thin film optics in the optical transmission measurement. The results of the two independent methods are in close agreement.

Keywords: Thermal conductivity; Optical properties; Thin film optics; Transmissivity; 3ω method; Amorphous silicon thin film

1. Introduction

Excimer laser melting and recrystallization is an efficient technology for obtaining high-performance polysilicon (p-Si) thin film transistors (TFTs) for applications in advanced flat panel displays. Since the recrystallized silicon morphologies are critically determined by complex phase transformations, it is important to analyze the transient temperature and the liquid–solid interface motion. The thermal conductivity is a key parameter that has to be known for this objective to be accomplished. The thermal conductivity of nearly perfect crystalline materials is well understood by assuming that heat is being carried by phonons that are weakly scattered by point defects and crystal boundaries. In contrast, for strongly disordered materials, the lack of lattice periodicity renders the microscopic description of heat transport difficult to achieve. The phonons with long mean free path does not contribute the heat transport due to the disorder in the material. Moreover, in the temperature range above 30 K, the conductivity rises smoothly to a limiting value, since the dominant high-energy vibrations are strongly scattered by local disorder [1].

The thermal conductivity of thin film is known as different that of bulk material due to the scattering of phonons at the boundary with the substrate. It depends on the film thickness as well as the fabrication method. The thermal conductivity is usually determined by obtaining the steady temperature gradient with known supplied heat flux. However, due to the geometrical restriction, i.e., the thin film, special techniques have been developed. There are two types to supply heat flux to the thin film. One is the direct heating method with fabricating electrical heater on the film such as the 3ω method. The other is the optical heating with a laser beam on the film. While heating up the sample, the temperature-dependent optical properties are measured such as reflectivity or transmissivity at the certain wavelength. The details of the latter method will be discussed further later. The 3ω method was an AC technique for measuring the thermal conductivity of bulk amorphous solids and crystals, as well as amorphous films in the temperature range from 30 to 750 K [2–4]. The advantage of this method is that it can minimize the radiation loss [4]. In the category of the latter

* Corresponding author. Tel.: +1-510-642-2525; fax: +1-510-642-6163.

E-mail address: cgrigoro@me.berkeley.edu (C.P. Grigoropoulos).

0017-9310/02/$ - see front matter
PII: S0017-9310(01)00347-7

Nomenclature

$2b$	metal line width
c_p	heat capacity
d	material thickness
f	frequency
I	laser intensity
I_c	electrical current
k	thermal conductivity
k_{ext}	extinction coefficient
l	metal line length
n	refractive index
R	resistance
R_{exc}	reflectivity at the excimer laser light wavelength
t	time
T	temperature
V	voltage
x	depth into the sample measured from the top film surface

Greek symbols

α	thermal diffusivity
γ	optical absorption coefficient
λ	wavelength
ρ	density
τ	characteristic time

Subscripts

f	thin film
s	substrate

methods, the photothermal, and non-contact method was developed to measure the thermal conductivity of silicon-dioxide layers on silicon [5]. In that experiment, the sudden temperature rise in the metal film was produced by a nanosecond laser pulse. The decay of the surface temperature was quantified by monitoring the optical reflectivity response to a probing HeNe laser. The temperature was compared with the result obtained from the conduction equation with the thermal conductivity producing the best fitting.

In the present work, the thermal conductivity of 53, 97, and 200 nm thick amorphous silicon (a-Si) films is measured by in situ optical transmission probing and compared by the results of the 3ω method. The advantages of the optical approach are that it is sample-preparation-free, and non-contact. The transient transmissivity is measured at the probe wavelength $\lambda = 633$ nm while the sample is heated with a KrF excimer laser ($\lambda = 248$ nm) of nanosecond pulse duration. Temperature-dependent optical refractive indexes are obtained by spectroscopic ellipsometry. The measured transmissivity is compared with the predicted response from thin film optics using measured temperature-dependent refractive indexes. The tempera- ture field can be deduced by solving the one-dimensional heat conduction equation for calculating the optical response in the thin film optics. The thermal conductivity can be determined as a fitting parameter in the comparison of the calculated response to the in situ experimental data.

2. Experimental procedures

2.1. Sample structure and the 3ω method

Undoped a-Si films of thickness 53, 97 and 200 nm were deposited by low pressure chemical vapor deposition (LPCVD) from Si_2H_6 on sapphire substrates at temperature 520 °C. The 53 and 97 nm thick films were deposited continuously. In contrast, the 200 nm thick film was deposited in three steps of $50 + 50 + 100$ nm with the wafer exposed to ambient environment between steps. In the 3ω method, a single thin metal line of width $2b$ and length l, serves as both heater and thermometer as shown in Fig. 1(a). Aluminum is evaporated to form the electrodes. A fraction of 2% Si is simultaneously deposited to prevent spiking of Al atoms into Si thin films. An ac driving current with angular frequency 1ω induces periodic heating at the frequency 2ω. Correspondingly, as the resistance of pure metals increases with temperature, these temperature oscillations produce an oscillation of the electrical resistance also at the frequency 2ω. Consequently, the voltage drop along the metal line has a 3ω component that can be used to measure the temperature distribution of the dielectric film and the substrate. The induced periodic temperature oscillation at the interface between the a-Si film and the substrate can be modeled in a manner identical to the standard formulation for bulk samples

$$\mathrm{d}T_s = \frac{P}{\pi l k_s}\int_0^\infty \frac{\sin^2(\mu b)}{(\mu b)^2(\mu^2+q^2)^{1/2}}\,\mathrm{d}\mu, \tag{1}$$

where

$$q^2 = \left(\frac{2\mathrm{i}\omega}{\alpha_s}\right). \tag{1a}$$

In the above, P is the power supplied to the line at the frequency 2ω, α_s is the thermal diffusivity and k_s is the thermal conductivity of the substrate. Eq. (1) is derived under the assumption that the heat enters the sample uniformly across the width of the metal line and that the metal line measures the average temperature of the substrate without altering the heat flow [3]. When the thermal conductivity of the thin film is small compared to that of the substrate, the thin film behaves as a simple

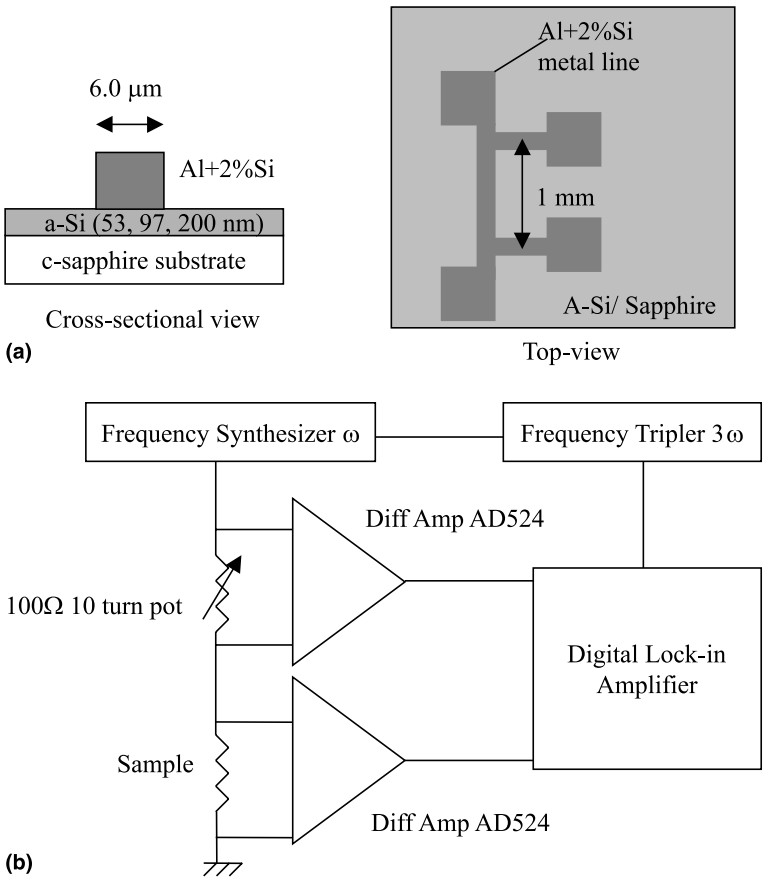

Fig. 1. (a) Sample structure for thin film thermal conductivity measurement using the 3ω method. (b) Schematic diagram of the equipment used for thermal conductivity measurements using the 3ω method.

thermal resistance, adding a frequency-independent temperature increment to dT_s (Eq. (1)) as follows:

$$dT_f = \frac{Pd_f}{2k_f bl}, \tag{2}$$

where k_f and d_f stand, respectively, for the thermal conductivity and thickness of the thin film. This simplification is valid when the thermal conductivity of the film is small compared to the thermal conductivity of the substrate. The 3ω method is ineffective if the substrate is glass, since the thermal conductivity of a-Si is expected to be of the same order as the thermal conductivity of glass. Crystalline sapphire (Al_2O_3) is therefore adopted as backing substrate, since its thermal conductivity is relatively high. The metal line was made of aluminum, with a 2% addition of silicon in order to prevent diffusion of silicon into the metal film.

Fig. 1(b) shows the schematic diagram of the bridge circuit used to measure the 3ω component of the voltage along the metal line. A digital lock-in amplifier produces not only the ac signal source, but also the 3ω reference signal. Since the amplitude of the 1ω voltage is typically 1000 times higher than the amplitude of the 3ω voltage, the third harmonic content in the source had to be entirely removed. The subtraction was accomplished using the differential input of the lock-in amplifier. The absolute error in the determination of the thermal conductivity caused by metal line size effects (i.e., width and thickness) and the dependence of the resistance on temperature (dR/dT) is estimated as 12%.

2.2. Transmission optical measurement

The schematic diagram of the experimental setup for measuring transmissivity is shown in Fig. 2. The a-Si thin film was heated by a KrF Excimer laser beam ($\lambda = 248$ nm) of 32 ns pulse length measured at full-width-half-maximum (FWHM). Fig. 3 shows the transient laser profile, obtained by capturing scattered excimer laser light on a silicon photodetector of $\sim$1 ns rise time. A tunnel-type beam homogenizer is used to ensure spatial uniformity of the laser beam. A quartz beam splitter is used to reflect 10% of the laser beam to an energy meter in order to measure the laser pulse energy.

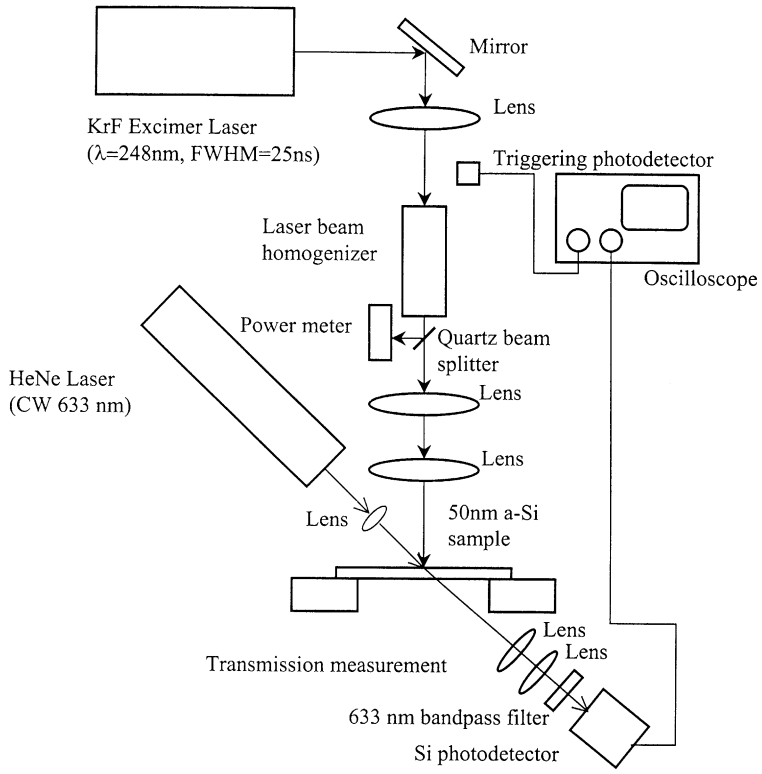

Fig. 2. Schematic diagram of the experimental setup for measuring transmissivity.

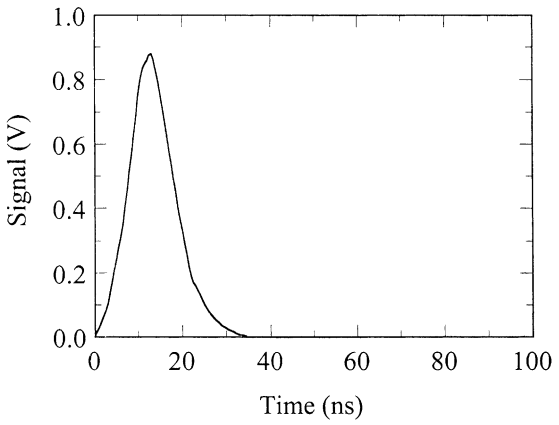

Fig. 3. Measured temporal laser pulse profile.

The excimer laser beam is focused onto the sample surface by two UV lenses. A probe HeNe laser beam ($\lambda = 633$ nm) focused onto the substrate at an angle of 45° with respect to the normal direction was used to measure the transient transmissivity during the heating process. A 633 nm narrow bandpass filter with half bandwidth of 50 nm is used to block stray excimer laser light. The measured transmissivity signal was normalized with the room temperature value obtained from thin film optics calculations [6] and direct measurement. To remove the inherent oscillation of the HeNe laser, Fast Fourier transformation is adopted. After normalization of the measured signal, the signal is transformed to the frequency domain. The signal is inversely transformed to the real time domain after the removal of the inherent oscillation components. Reflectivity could also be chosen as a measuring parameter, especially for thin films on opaque substrates since its magnitude also depends on the transient temperature variation. However, the sensitivity of the transmissivity at the wavelength of 632.8 nm is better than that of the reflectivity by 14.3% compared to 7.2% for a 300 K temperature increase.

3. Numerical calculation of the transient optical response

The schematic diagram for the numerical modeling is displayed in Fig. 4(a). The laser beam spot size on the target is 5.9×1.9 mm^2, while the penetration depth of the temperature profile within the laser pulse duration is less than 1 μm. Therefore, it can be assumed that the heat transfer at the center of the laser beam is essentially one-dimensional. The conductive heat transfer, both in the thin film and the substrate is given by

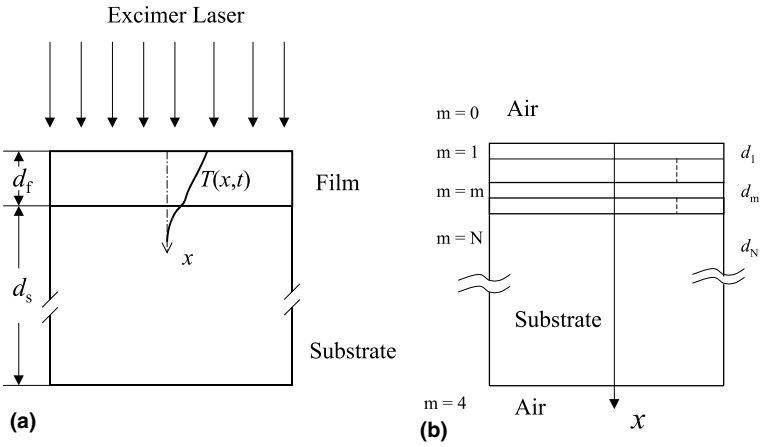

Fig. 4. (a) Schematic diagram for the numerical model, and (b) for the thin film optics calculation.

$$\rho c_p(T)\frac{\partial T}{\partial t} = \frac{\partial}{\partial x}\left(k\frac{\partial T}{\partial x}\right) + (1 - R_{exc})I(t)\gamma\exp(-\gamma x), \quad (3)$$

where R_{exc} is the normal reflectivity at the wavelength of 248 nm and γ the optical penetration depth ($=\lambda/4\pi k_{ext}$). The nanosecond pulsed laser energy is treated as an internal energy source, considering that the time for photon energy transfer is much faster than the time for conductive heat transfer in the solid. The temporal profile of excimer laser presented in Fig. 3 is adopted for the laser heating source $I(t)$. The boundary conditions and the initial condition in the thin film and the sapphire substrate are as follows:

$$\left.\frac{\partial T}{\partial x}\right|_{x=0} = 0, \quad (4a)$$

$$T(x = d_f + d_s, t) = T_\infty, \quad (4b)$$

$$T(x, t = 0) = T_\infty. \quad (4c)$$

The time scale, O (40 ns), in this problem is so small that convection and radiation losses from the top of the surface to the environment are negligible. Thus, the adiabatic boundary condition can be applied at the thin film surface. During the laser heating process, the temperature penetration depth into the substrate is small, O (1 μm), compared with the thickness of the wafer (600 μm). The bottom substrate surface can therefore be safely assumed to remain at the ambient temperature. The uniform grids are placed in the thin film. The dense grids are put on the boundary of the film in the substrate.

To obtain the reflectance and transmittance of the entire thin film system including the substrate, the thin film optics formulation is applied. Using the formalism of the characteristic transmission matrix [6], the lumped structure reflectivity can be obtained [7,8]. The schematic diagrams for optical modeling discussed at the previous section are presented in Fig. 4(b).The structure is assumed to have N layers, starting from 1. The s-polarized HeNe lasers are used for probing purpose. Thus, the following formulation is based on s-polarized light, i.e., transverse electric (TE) wave. For s-polarized light, the mth layer of thickness d_m, with a complex refractive index, $\hat{n}_m = n_m + \mathrm{i}\cdot k_m$ is represented by the 2×2 matrix M_m, whose elements are complex

$$M_m = \begin{bmatrix} \cos\left(\frac{2\pi}{\lambda}p_m d_m\right) & \frac{\mathrm{i}}{p_m}\sin\left(\frac{2\pi}{\lambda}p_m d_m\right) \\ \mathrm{i}p_m\sin\left(\frac{2\pi}{\lambda}p_m d_m\right) & \cos\left(\frac{2\pi}{\lambda}p_m d_m\right) \end{bmatrix}, \quad (5)$$

where

$$p_m = \hat{n}_m\cos\hat{\theta}_m. \quad (5a)$$

The complex angle of incidence, $\hat{\theta}_m$ can be acquired from generalized Snell's law

$$\sin\theta_i = \hat{n}_m\sin\hat{\theta}m. \quad (6)$$

The multi-layer transmission matrix, M, is

$$M = \prod_{m=1}^{N} M_m. \quad (7)$$

The reflection and transmission Fresnel coefficients, r_F and t_F, are

$$r_F = \frac{[M(1,1) + M(1,2)p_N]p_1 - [M(2,1) + M(2,2)p_N]}{[M(1,1) + M(1,2)p_N]p_1 + [M(2,1) + M(2,2)p_N]}, \quad (8)$$

$$t_F = \frac{2p_1}{[M(1,1) + M(1,2)p_N]p_1 + [M(2,1) + M(2,2)p_N]}. \quad (9)$$

The structure reflectivity, R, and transmissivity, τ, in terms of r and t follows:

$$R = |r_F|^2, \quad (10)$$

$$\tau = \mathrm{real}(p_N/p_1)|t_F|^2. \quad (11)$$

The structure size parameters and thermal properties used in the calculations are given in Table 1. Furthermore, the temperature dependence of the thermal conductivity and heat capacity of sapphire is given in Table 2 [9,10]. Thin film optics theory is used to derive the optical properties of the sample structure. The temperature field in the amorphous silicon thin film induces changes in the material refractive index. Thus, the thin film is treated as a stratified multilayer structure, defined by the grid division used in the finite difference numerical calculation.

The optical properties of the a-Si film were measured by spectroscopic ellipsometry using the experimental apparatus [11]. The acquired optical properties are as follows:

(i) $\lambda = 248$ nm

$$\begin{aligned} n &= 1.5175 + 0.0017642T \\ k &= 3.2564 + 0.00050947T \end{aligned} \quad (298\ \text{K} \leqslant T \leqslant 671\ \text{K}), \tag{12}$$

(ii) $\lambda = 633$ nm

$$\begin{aligned} n &= 4.3506 + 0.00060589T \\ k &= 0.041329 + 0.0007398T \end{aligned} \quad (298\ \text{K} \leqslant T \leqslant 671\ \text{K}). \tag{13}$$

For the sapphire substrate [12]

$$\hat{n} = 1.7662 + \mathrm{i} \cdot 0 \quad (T = 300\ \text{K}) \tag{14}$$

is used over the entire temperature range.

Table 1
Parameters and thermophysical properties of sapphire and a-Si

Density of sapphire, ρ_s	3970 kg/m^3
Density of a-Si, ρ_f	2330 kg/m^3
Heat capacity of amorphous silicon thin film, c_{pf}	992 J/kg K
Substrate temperature	300 K
Initial temperature, T_i	300 K
Amorphous silicon film thickness, d_f	53, 97 and 200 nm
Sapphire substrate thickness, d_s	600 μm

Table 2
Thermal conductivity and heat capacity of sapphire [9,10]

Temperature (K)	Thermal conductivity, κ_s (W/mK)	Heat capacity, c_{ps} (J/kg K)
300	46.0	765
400	32.4	940
600	18.9	1110
800	13.0	1180
1000	10.5	1225

4. Results and discussion

4.1. Thermal conductivity via the 3ω method

The thermal conductivity of the bare sapphire substrate was first determined for the purpose of testing the measurement setup. In the 3ω technique, the in-phase and out-of-phase components of temperature oscillations, $\mathrm{d}T_s$ generated on a metal line directly deposited on the sapphire substrate are measured. The in-phase component corresponds to the real part of the temperature response, whereas the out-of-phase represents the imaginary part. The temperature oscillations were calculated using

$$\mathrm{d}T_s = 2\frac{\Delta T}{\Delta R}\frac{R}{V}V_{3\omega}, \tag{15}$$

where R is the average resistance of the metal line, V is the rms voltage across the metal line at the first harmonic (frequency 1ω) and $V_{3\omega}$ the measured rms amplitude of the voltage at the 3ω frequency. The change of the resistance of the metal line with respect to temperature and hence the calibration factor $\Delta R/\Delta T$ was measured statically by heating the sample in an oven. The thermal conductivity can be determined on the basis of either the in-phase or the out-of-phase oscillation amplitudes. The thermal conductivity k_s is given by

$$k_s = \frac{\Delta R}{\Delta T}\frac{V^3 \ln(f_2/f_1)}{4\pi l_c R^2 (V_{3\omega,1} - V_{3\omega,2})}, \tag{16}$$

where $V_{3\omega,1}$ and $V_{3\omega,2}$ are the rms 3ω voltage amplitudes at the frequencies f_1 and f_2 correspondingly [3]. The in-phase amplitudes yielded thermal conductivity, $k_s = 43.2$ W/mK and the out-of-phase 42 W/mK. The thermal conductivity of the sapphire substrate [10] is 46 W/mK at $T = 300$ K. The measured values have the error of 8.7%. Fig. 5(a) shows 3ω signals obtained from the a-Si on sapphire substrate samples for a metal line width, $2b = 6$ μm. As expected on the basis of Eqs. (4a)–(4c), the presence of the a-Si thin film produces a frequency-independent increase on the amplitude of the in-phase temperature oscillations. The thermal conductivity of the 53 and 97 nm a-Si films shown in Fig. 5(b) is about 1.5 W/mK, which is by about 100 times smaller than the thermal conductivity of crystalline silicon (c-Si) (~150 W/mK at room temperature). The measured thermal conductivity of the 200 nm film is about 2.2 W/mK. This discrepancy is due to the different deposition procedure for the thicker film, which may affect the film quality since the thermal conductivity of amorphous materials is not dependent on thickness.

4.2. Thermal conductivity via the optical transmission method

Fig. 6 shows the corresponding measured transient transmissivity trace induced by the excimer laser fluence

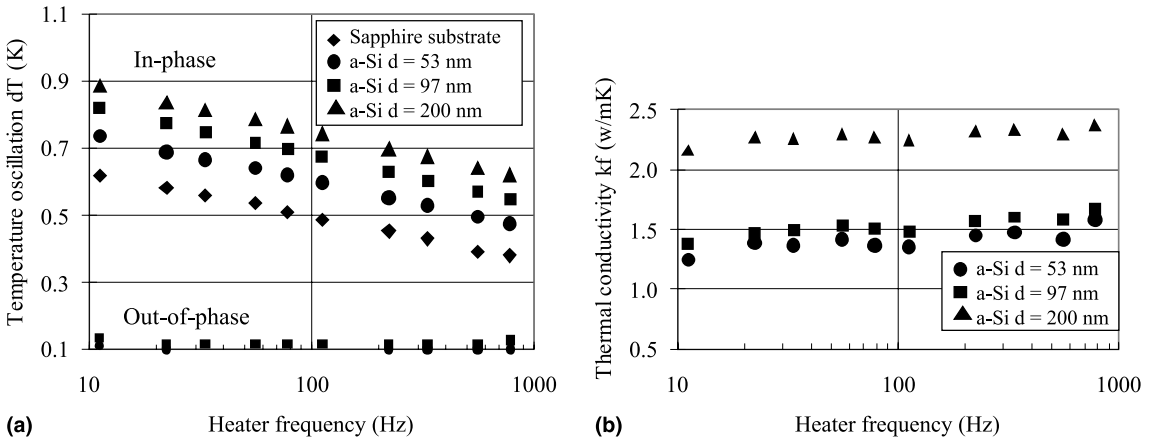

Fig. 5. The 3ω method results for the a-Si film/sapphire substrate structure (the metal line width is 6 μm): (a) amplitudes of temperature oscillations for the a-Si sapphire substrate, (b) thermal conductivity of the a-Si film.

of 44 mJ/cm^2 and the calculated transmissivity traces with three different thin film thermal conductivities in the 53 nm thick a-Si films. The computed transmissivity responses reveal a clear dependence on thermal conductivity. In evaluating the transmissivities, the transmissivity is averaged over its interference period with the variation of the substrate thickness, since the thickness of the substrate, 600 μm, is much larger than the probing laser beam wavelength of 633 nm. The transmission response calculated using the thermal conductivity value of 1.5 W/mK fits the measured transmissivity best. To check the validity of the calculation, the transient surface temperatures are obtained as shown in Fig. 7. The measured optical properties are in the temperature range from 298 to 671 K. The maximum temperature is around 690 K at $t = 16$ ns with $k = 1.5$ W/mK. It shows 2.8% deviation from the measured data temperature range. The linear extrapolation is used to obtain the refractive index outside the measured temperature

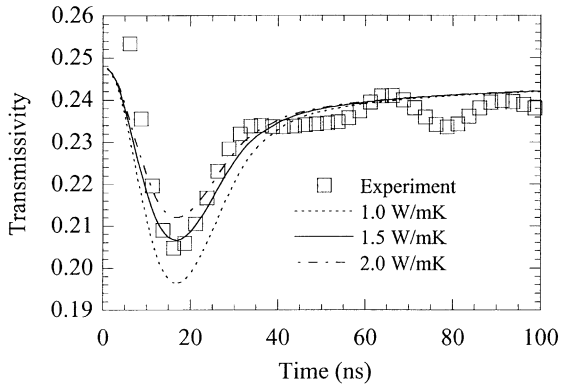

Fig. 6. Comparison of measured transmissivity and calculated transmissivity traces for the excimer laser fluence of 44 mJ/cm^2 incident on the 53 nm-thick film.

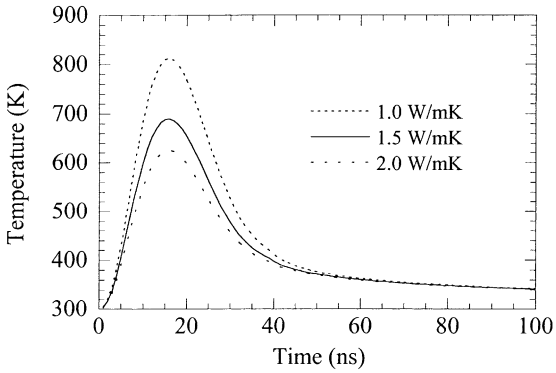

Fig. 7. Transient surface temperature evolutions for different values of the 53 nm-thick a-Si film thermal conductivity for the excimer laser fluence of 44 mJ/cm^2.

range. As the thermal conductivity is smaller, the deposited heat tends to be confined in the surface and produces the higher surface temperature. Fig. 8 presents the transient temperature profiles in the 53 nm film and the adjacent part of the substrate for the excimer laser fluence of 44 mJ/cm^2. The temperature profiles are calculated using thermal conductivity of 1.5 W/mK for the a-Si film. From scaling analysis, it is estimated that the characteristic length of heat diffusion in the solid thin film attained over the duration of the laser pulse of 40 ns, $(4k_f\rho_f^{-1}c_{pf}^{-1}\tau)^{1/2}$, is O (320 nm). During the laser heating, the deposited heat cannot be confined the film. The heat starts to be diffused away to the substrate. And the length of heat affected zone increases. The steep temperature gradients induced in the thin film due to the low thermal conductivity impart significant change of the film optical properties.

Fig. 9 shows the corresponding measured transient transmissivity trace induced by the excimer laser fluence

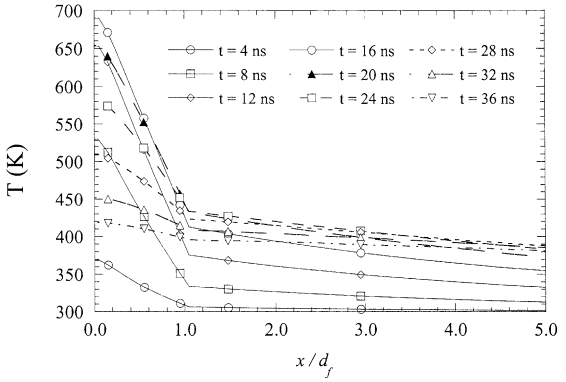

Fig. 8. Transient temperature profiles in the 53 nm thick film and the adjacent substrate with an excimer laser fluence of 44 mJ/cm^2 ($k_f = 1.5$ W/mK).

of 43 mJ/cm^2 and the calculated transmissivity profiles with various thermal conductivities in the 97 nm thick films on the sapphire substrate. In the 97 nm thick films, the transmission response calculated using the thermal conductivity value of 1.5 W/mK also follows the measured transmissivity best. The transient surface temperatures are obtained as shown in Fig. 10. The maximum temperature is around 807 K at $t = 17$ ns with $k_f = 1.5$ W/mK. It exceeds 20.2% from the measured data temperature range. The linear extrapolation is also adopted to obtain the refractive index outside the measured temperature range. As the thermal conductivity is smaller and the film is thicker, the surface temperature is higher. Fig. 11 shows that the best fitting to the measured transmissivity trace for the 200 nm film exposed to a fluence of 53 J/cm^2 is close to 2.2 W/mK. The discrepancy might be induced from the different type of the fabrication method as mentioned above. Thus, the temperature-dependent refractive indexes can be slightly

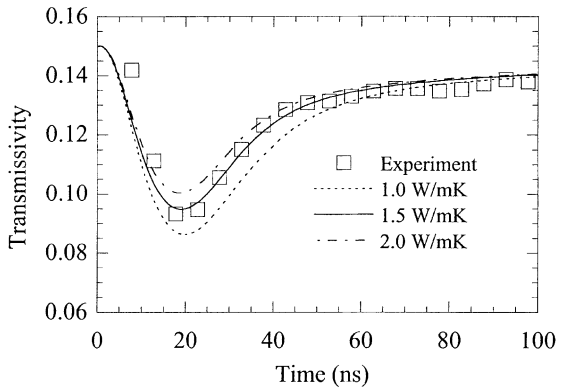

Fig. 9. Comparison of measured transmissivity and calculated transmissivity traces for the excimer laser fluence of 43 mJ/cm^2 incident on the 97 nm thick film.

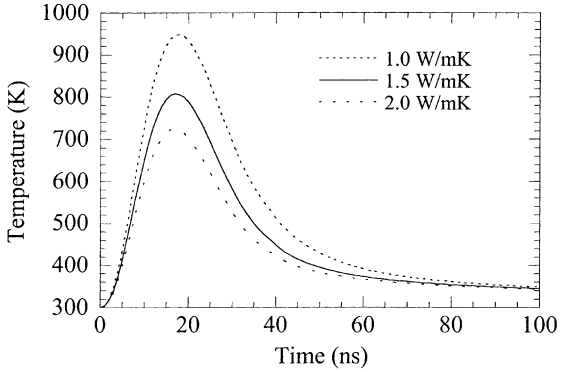

Fig. 10. Transient surface temperature evolutions for different values of the 97 nm thick a-Si film thermal conductivity for the excimer laser fluence of 43 mJ/cm^2.

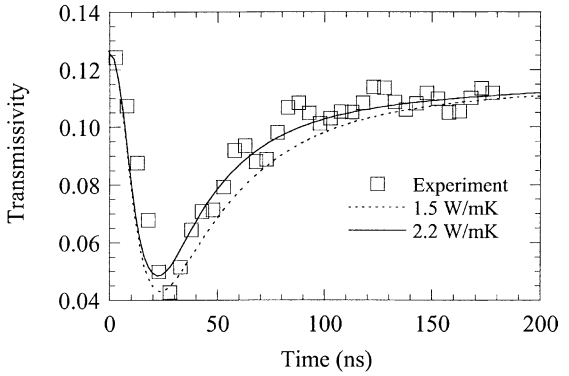

Fig. 11. Comparison of measured transmissivity and calculated transmissivity traces for the excimer laser fluence of 53 mJ/cm^2 incident on the 200 nm thick film.

changed. It is therefore confirmed that the optical method yields results in good agreement with the 3ω method. Cahill et al. [2] measured the thermal conductivity of a-Si:H film as 1.1 W/mK at 300 K. Due to the disorder of amorphous silicon, the dominant high-energy vibrations are so strongly scattered by local disorder. It is known that temperature dependence in the high temperature is slight [1].

5. Conclusion

The thermal conductivity of a-Si thin films was determined by in situ optical measurement as well as by the 3ω method. The optical measurement has advantages of no sample preparation and simple technique. For the thin film optics calculation of transmission, the thin film complex refractive index was also determined by spectroscopic ellipsometry according to the temperature

variance. The acquired transmission signal was fitted with predictions obtained by coupling a conductive heat transfer equation with multi-layer thin film optics. The results of the two independent methods were in close agreement. The discrepancy of the thermal conductivity of 200 nm with 53 and 97 nm was believed to be caused by the fabrication procedure, not by the thickness difference.

Acknowledgements

This work was supported by the Hitachi, Japan. The 53 nm thick a-Si thin films were provided by the Hitachi, Japan. We also thank Professor David G. Cahill for advising on the 3ω method.

References

[1] P.B. Allen, J.L. Feldman, Thermal conductivity of glasses; theory and application to amorphous Si, Phys. Rev. Lett. 62 (1989) 645–648.
[2] D.G. Cahill, M. Katiyar, J.R. Abelson, Thermal conductivity of a-Si:H thin films, Phys. Rev. B 50 (1994) 6077–6081.
[3] D.G. Cahill, Thermal conductivity measurement from 30 to 750 K: the 3ω method, Rev. Sci. Instrum. 61 (1990) 802–808.
[4] D.G. Cahill, R.O. Pohl, Thermal conductivity of amorphous solids above the plateau, Phys. Rev. B 35 (1987) 4067–4073.
[5] O.W. Käding, H. Skurk, K.E. Goodson, Thermal conduction in metallized silicon-dioxide layers on silicon, Appl. Phys. Lett. 65 (1994) 1629–1631.
[6] M. Born, E. Wolf, Principles of Optics, sixth ed., Cambridge University Press, Cambridge, 1980.
[7] C.P. Grigoropoulos, H.K. Park, X. Xu, Modeling of pulsed laser irradiation of thin silicon layers, Int. J. Heat Mass Transfer 36 (1993) 919–924.
[8] H.K. Park, X. Xu, C.P. Grigoropoulos, N. Do, L. Klees, P.T. Leung, A.C. Tam, Temporal profile of optical transmission probe for pulsed-laser heating of amorphous silicon films, Appl. Phys. Lett. 61 (1992) 749–751.
[9] Y.S. Touloukian, R.W. Powell, C.Y. Ho, P.G. Klemens, in: Thermophysical Properties of Matter; Thermal Conductivity: Nonmetallic Solids, vol. 2, IFI/Plenum, New York-Washington, 1970.
[10] Y.S. Touloukian, E.H. Buyco, in: Thermophysical Properties of Matter; Specific Heat: Nonmetallic Solids, vol. 5, IFI/Plenum, New York, Washington, 1970.
[11] B.K. Sun, X. Zhang, C.P. Grigoropoulos, Spectral optical functions of silicon in the range of 1.13–4.96 eV at elevated temperatures, Int. J. Heat Mass Transfer 40 (1997) 1591–1600.
[12] E.D Palik, Handbook of Optical Constants of Solids, Academic Press, New York, 1985.